

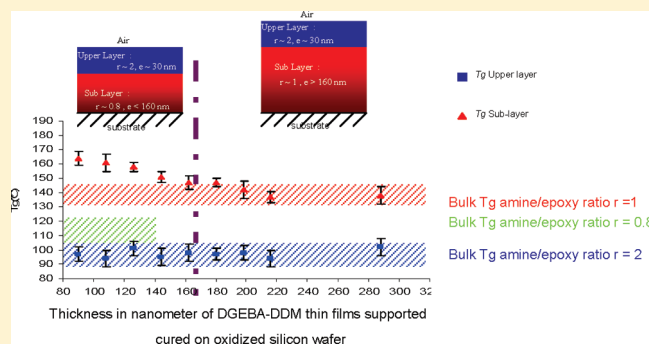
# Nanostructuration in Thin Epoxy–Amine Films Inducing Controlled Specific Phase Etherification: Effect on the Glass Transition Temperatures

Sandra Onard, Isabelle Martin, Jean-Francois Chailan, Alain Crespy, and Pascal Carriere\*

Laboratoire des Matériaux, Polymères, Interfaces et Environnement Marin (MAPIEM), Faculté des Sciences et Techniques, Université du Sud Toulon Var, Avenue de l'Université, 83 957 La Garde Cedex, France

**S** Supporting Information

**ABSTRACT:** In order to prepare cured thin films thicknesses in the range of 90–300 nm, epoxy–amine mixtures of different concentrations in toluene are spin-cast onto oxidized silicon substrates. The glass transition temperature of the cured thin films is measured by microthermal analysis, revealing the existence of two distinct glass transitions temperatures for all the samples due to amine segregation at air/film interface. These transitions are ascribed to two layers. The upper layer properties of the film due to the air/polymer interface are independent of the film thickness. This layer is around 30 nm thick, and its glass transition temperature is about 97 °C and matches to a constant amine/epoxy composition at the air/film interphase. Consecutively, the film thickness reduction induces an increase of the epoxy excess in the sublayer, promoting side epoxy reactions revealed by aliphatic ether bonds formation. Thus, significant increase of the sublayer  $T_g$ , in comparison to the  $T_g$  of the bulk sample with an equivalent amine/epoxy ratio at the same amine conversion rate, is mainly due to these new ethers bonds for film thickness less than 160 nm. These bonds, surface catalyzed, are created at low temperature by the consumption of the epoxy excess. Etherification enhancement is finely controlled by the amine–epoxy off stoichiometry in the sublayer tuned by its thickness and mainly results in glass transition temperature increase at lightly amine conversion. At complete epoxy and high amine conversion reached by postcuring, etherification in the sublayer leads to a constant amount whatever the thickness of the sample. The glass transition temperature of the sublayer postcured is around 180 °C, equivalent to the bulk sample and does not bring out confinement effects.



Along with the expansion of nanotechnology, thin polymer films are currently used, for example as resists, interlayer dielectrics, or lubricants, and can determine the properties of some devices<sup>1</sup> as well as adhesives and coatings, fiber-reinforced composites,<sup>2,3</sup> nanocomposites, artificial tissues scaffolds, or electronics packaging. Even though understanding the relationships between network structure and surface and interface properties of thermosetting resins is a subject of great interest, it is still unclear. According to cross-linked polymer thin films, little studies were carried out to tackle potential confinement effect or quantitative interface effect on network structure near the solid surface.

For thermoset films, Wang and Zhou studied the glass transition temperature ( $T_g$ ) of the microtome-sliced epoxy thin film<sup>4</sup> from a fully cured bulk sample. The  $T_g$  was found to decrease with film thickness, and a  $T_g$  depression of 15 K was observed for a 40 nm thin film as compared with the bulk sample. They ascribed this reduction to the finite size of the sample and the predicted downward shift of critical temperature in 2D against 3D system avoided hypothesis of kinetics and reptation dynamic influence on the glass transition reduction in confined film. More recently, Li

and Simon<sup>5</sup> have found that nanoconfinement had significant effect on the glass transition temperature reduction of thermoset matrices in controlled pore glass without any change on the network structure upon nanoconfinement. Unlike confinement in pores, the glass transition temperature deviation of thin films supported on  $\text{SiO}_x$  substrates is smaller and depends on the substrate/polymer interactions.<sup>6–10</sup> Nevertheless, for thin thermosetting films supported on silicon surface, Lenhart<sup>11</sup> had shown that deviation on the expansion coefficients at the rubbery state from bulk to confined thermoset films occurred in the range 20–40 nm film thickness whatever the surface treatment used modifying surface energy and polymer/surface interactions. He assumed that the cross-linked network had a significant influence on the thin film thermal behavior and can screen the polymer/surface interactions. Preventing segregation phenomenon, Lenhart assumes a homogeneous network cross-link density. Thus,

**Received:** September 2, 2010

**Revised:** January 28, 2011

**Published:** April 04, 2011



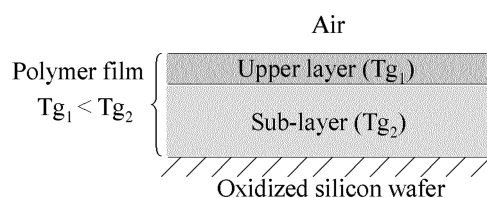


**Figure 1.** Schematic representation of the stratification in epoxy-diamine films (film thickness  $\sim 200$  nm).

the length scale of confined behavior would be reduced to 5 nm from the substrate.

Concerning epoxy-amine resins directly cured in the presence of a solid surface, several workers have suggested that the stoichiometry and the curing process were affected at the solid surface and led to the formation of an organic/inorganic interfacial region of which the structure and the properties differed from the bulk resin.<sup>12</sup> According to Palmese and McCullough, the knowledge of the interfacial stoichiometry enables to estimate the interphase properties through a calibration with the bulk resin properties as a function of composition.<sup>13,14</sup> Although some studies on ultrathin thermosetting films had focus on preferential segregation at the solid silicon substrate/polymer network interface,<sup>15</sup> no more than an epoxy monolayer of reduce mobility could be shown by neutron reflectivity at this interface. Yim et al.<sup>16</sup> also reported that the composition modification at polymer/substrate interface is limited to a few angstroms, whereas they noticed a great enrichment of cross-linker at the air/polymer interface for 80 nm thin films. These segregation phenomena strongly affect the polymer network structure in the film thickness by creating two distinguishable layers (Figure 1) with different cross-link density. Recently, we have highlighted that this preferential segregation in thermoset supported films of 200 nm thick was at the origin of two glass transition temperatures measured by microthermal analysis<sup>17</sup> and dynamic mechanical analysis. Moreover, the amine segregation process does not seem to depend neither on the initial stoichiometry of the amine/epoxy mixture<sup>16</sup> nor on the surface chemistry.<sup>17</sup> The amine/epoxy segregation in the film seems to be mainly controlled by surface tension at the air/polymer interface.

Thus, using these properties and keeping the whole amine/epoxy ratio constant allow us to tune the amine/epoxy ratio in the sublayer by reducing films thickness and by controlling amine consumption. Therefore, the Palmese and McCullough approach for understanding the polymer network properties near an interface, focusing on the determination of the chemical composition profile of the resin monomers near the surface, is still relevant to thin film with thicknesses in the range of 40–200 nm. The resulting macromolecular mobility of the two polymer layers will thus be determined by microthermal analysis used as thermomechanical analysis which is quite sensitive to the cross-link density.<sup>18,19</sup> We will try to answer whether the glass transition temperature of the different sublayers from 60 to 270 nm can be predicted easily from their initial stoichiometry, taking the bulk resin properties as reference, or if surface and confinement effect influence glass transition of thermosetting thin films.

## METHODS

**Materials.** The epoxy resin based on diglycidyl ether of bisphenol A (DGEBA) was purchased from Hempel with a molar mass of 385 g/mol

( $n = 0.16$ ) and cured with 4,4'-diaminodiphenylmethane (DDM) purchased from Sigma-Aldrich (99.9%).

Silicon wafers (100) were purchased from Mat Technology, immersed in a piranha solution for 30 min at 70 °C, rinsed with deionized water, and dried under a flow of argon. Thermal cure thin films were carried out using a VWR model 400 temperature-controlled hot plate in air.

**General Procedures.** Thin supported polymer films used in this study were produced by spin-coating a toluene solution of DGEBA-DDM mixture on oxidized silicon wafers. The solution mixtures are characterized by the ratio  $r$  of amino hydrogen to epoxide  $r = [\text{NH}]/[\text{EP}]$ . For the stoichiometric mixture of two DGEBA molecules to one diamine molecule,  $r = 1$ . In this study, the ratio chosen for all the solution is 1.13. Then, the samples were degassed under vacuum at room temperature for 15 min. No more residual solvent can be observed on FT-IR spectra of thin films (see Supporting Information). Samples are cured at atmospheric pressure according to the following schedule (named stage 1): 1 h at room temperature, 1 h at 50 °C, 45 min at 75 °C, and 30 min at 110 °C.

The concentration of the epoxy solution varied between 25 and 80 g L<sup>-1</sup> in order to obtain homogeneous thin films with thicknesses from 90 to 300 nm. A detailed discussion of the sample preparation is given elsewhere.<sup>17</sup> An additional postcuring of 2 h at 180 °C is applied to the sample after first microthermal and infrared characterizations to complete epoxy conversion.

**Microthermal Analysis for the Local Glass Transition Determination.** Local glass transition temperature measurements were carried out on a TA Instruments 2990 microthermal analyzer ( $\mu$ TA). Probe temperature calibration was performed using room temperature and the DSC (differential scanning calorimetry) peak melting point of poly(ethylene terephthalate) (PET). Using the  $\mu$ TA localized thermal analysis (L-TA) mode, the probe was held in place at a location selected on the surface, with a force of 12 nA and its temperature was usually raised from 25 to 250 at 15 °C s<sup>-1</sup> and then cooled to 25 °C. The vertical position of the probe during heating was followed by laser displacements focus on the probe (L-TMA, localized thermomechanical analysis or sensor signal).<sup>20,21</sup> The probe was then moved of 10  $\mu$ m between each L-TA measurement in order to make sure that each microthermal analysis was not perturbed by the previous ones.

**Infrared Reflection Absorption Spectroscopy (IRRAS).** IR-RAS spectra were obtained using a FTIR spectrometer Thermo Nicolet Nexus. All spectra were recorded at an incidence angle of 50° in order to analyze the whole thickness of polymer films.<sup>22,23</sup> 600 scans were recorded at a resolution of 4 cm<sup>-1</sup>. A cleaned silicon wafer was used as reference spectrum. FT-IRRAS allows us to check that the amine/epoxy ratio of all the films before cure remained constant and corresponded to the initial amine/epoxy ratio in solution. The spin-coating process does not remove preferentially one of the reactive components. FT-IRRAS is also used to determine the epoxy and primary amine consumption after cure and postcure.

## RESULTS AND DISCUSSION

The results of some L-TA measurements made on thin supported epoxy/diamine films cured at 110 °C with different thicknesses are shown in Figure 2.

A close inspection of the sensor signal obtained shows the presence of two glass transition temperatures whatever the thickness of polymer films partially cured. Therefore, we can consider that the stratification of thin epoxy/diamine films in two layers<sup>16</sup> with different stoichiometry and different cross-link density<sup>17</sup> takes place for the different films analyzed. Figure 3 plots the glass transition temperatures for the two polymer layers as a function of the film thickness.

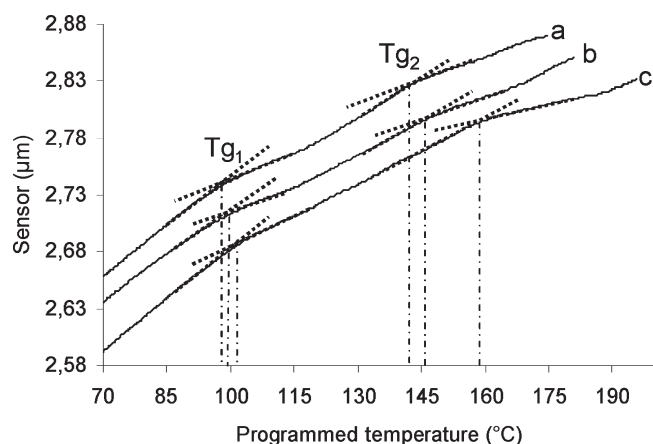


**Figure 2.** Sensor height position response versus temperature for thin polymer films of different thicknesses (a, 200 nm; b, 160 nm; c, 126 nm) and cured according to the stage 1 (i.e., without postcure at 180 °C).

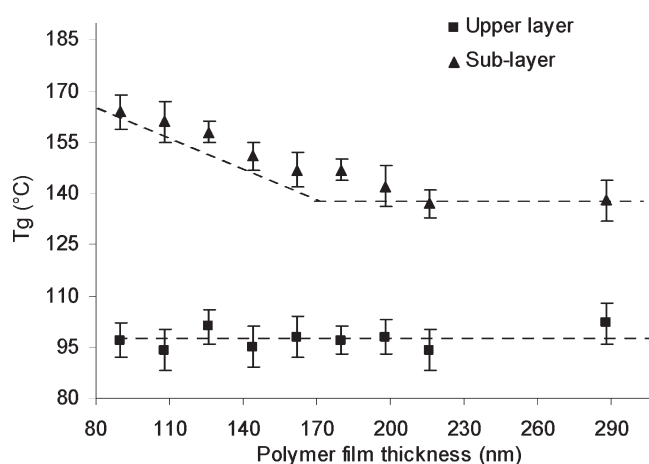


**Figure 3.** Glass transitions evolution for the two polymer layers after curing (stage 1) as a function of the epoxy–diamine film thickness.

The lower glass transition temperature ascribed to the upper layer is constant whatever the thickness of the film whereas the glass transition temperature of the sublayer increases with thickness reduction.

• **The Upper Layer Properties.** The  $T_g$  of the layer at the air/network interface remains close to 97 °C and is also independent of the polymer film thickness. The thickness of the upper layer is calculated from  $\mu$ TA measurements as the step height at half-height between the extrapolated tangents following procedure described in detail elsewhere.<sup>24</sup> Thus, the upper layer thickness is estimated to be roughly 30 nm for both samples. Segregation of amine to air surface is expected on the basis of the surface tensions of the DGEBA (48.7 mJ/m<sup>2</sup>) and the DDM (28 mJ/m<sup>2</sup>). Segregation of low surface energy components at air surface has been studied extensively in other multicomponents polymer films.<sup>16,25,26</sup> Moreover, we have previously showed that cross-linking and mobility of this film at the air/network interface were neither affected by the substrate surface nor modified by postcure.<sup>17</sup> In order to estimate the stoichiometry in the upper layer, we take the bulk resin as reference and estimate its stoichiometry from its  $T_g$ . A glass transition of 100 °C corresponds to an amine/epoxide ratio of 2. The L-TA measurements

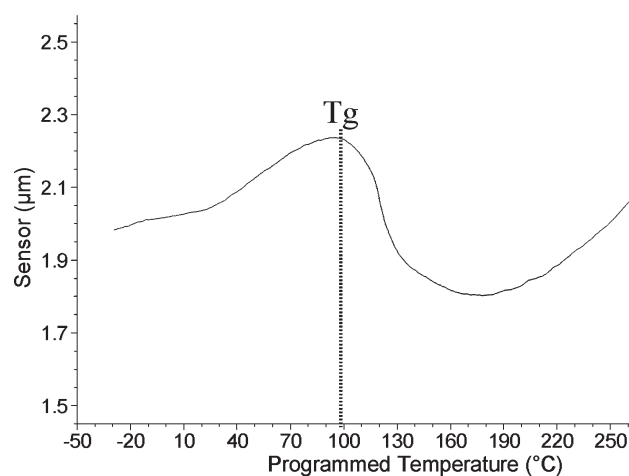


**Figure 4.** Sensor height position response versus temperature for the bulk DGEBA–DDM resin (amine/epoxide ratio of 2) cured according to the stage 1.

made on the bulk DGEBA–DDM resin, prepared with this amine/epoxide ratio and cured according to the same heating schedule (stage 1) used for thin films show only one glass transition at a temperature of  $99 \pm 8$  °C (Figure 4).

Microthermal analysis on the bulk sample does not reveal any evidence of a thin layer with a reduce glass transition due to free surface or specific orientation at this interface. Torkelson et al.<sup>27</sup> have shown that free surfaces decrease the  $T_g$  in ultrathin PMMA films relative to bulk PMMA. Nevertheless, our films are not thin enough and have not large surface-area-to-volume ratio as compared with Torkelson thin films geometry to undergo a 40 K reduction on  $T_g$  as we have measured by microthermal analysis. The  $T_g$  of the upper layer is close to 100 °C; we thus suggest that initial amine/epoxide ratio in the upper layer is close to 2 whatever the thickness of polymer films. In the upper layer amine-rich side, all epoxide groups on the network structure are supposed to have reacted completely. No glass transition temperature modification in this layer is observed after postcure treatment at 180 °C for 2 h.

The stoichiometry and the thickness of the upper layer are comparable for all the polymer films. It seems that during the synthesis the amount of amine functions migrating to the air/film interface is nearly constant whatever the thickness of polymer films analyzed. This layer stratification is mainly controlled by the differences in surface tensions of the components and the evaporation rate of the solvent during spin-coating. The cross-linking of the upper layer is performed with the same cure schedule, stoichiometry, and thickness, so the upper layer is supposed to have the same average mechanical and thermal properties for all the polymer films.

• **The Sublayer Properties.** Unlike the upper layer, the  $T_g$  of the sublayer is significantly affected by the film thickness and increases with the thinning of polymer films (Figure 3). Assuming that stoichiometry and thickness of the upper layer are independent of the film thickness, the conservation of matter in the whole film affords us to assume both variations of the stoichiometry and thickness of the sublayer. As the whole film thickness decreases, the sublayer thickness decreases and the excess epoxides functions relative to amine ones increases in parallel. Mass balance in the sublayer is used to quantify amine/epoxy ratio versus the film thickness which is illustrated in Figure 5.

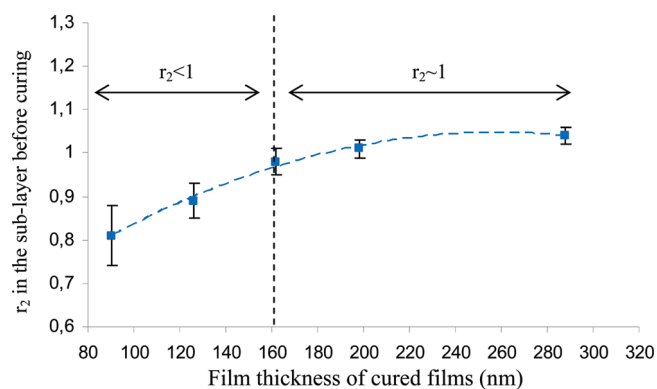


**Figure 5.** Amine/epoxy ratio ( $r_2$ ) in the sublayer as a function of the film thickness before curing.

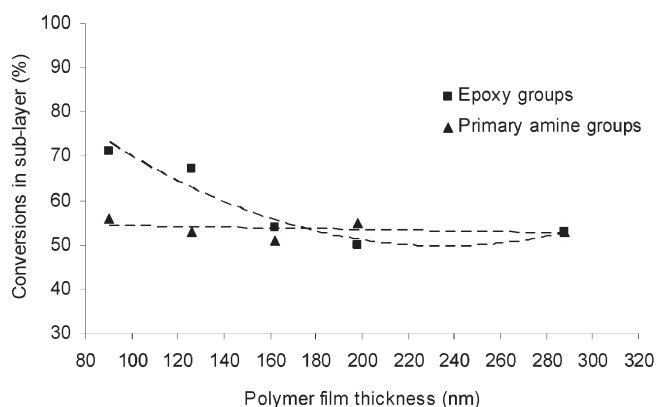


**Figure 6.** Conversion of the epoxy and primary amine groups in the sublayer after curing according to the stage 1 (i.e., without postcure at 180 °C) as a function of the film thickness.

The amine/epoxy ratio reaches 0.9–0.8 in the sublayer before curing since the film thickness gets less than 160 nm. In bulk resins, the highest  $T_g$  is obtained for amine/epoxide ratio close to 1 and decreases on either side of stoichiometry.<sup>28,29</sup> In the case of epoxy-rich samples, the decrease of  $T_g$  is generally attributed to dangling epoxy molecules which increase free volume of resin. Surprisingly, the epoxy consumption increases as the thickness decreases (Figure 6) whereas primary amine consumption remains constant with the film thickness.

**Influence of the Network Structure on the Sublayer Glass Transition.** The FT-IRRAS spectra of partially cured films in Figure 7 show that the intensity of the 1120  $\text{cm}^{-1}$  band, corresponding to the aliphatic ether linkages, significantly increases during curing of polymer films thinner than 160 nm. Thus, the etherification/homopolymerization reactions are favored in thin films (thickness < 160 nm), i.e., when the sublayer is initially, before curing, in excess of epoxides. In bulk resins, it is supposed that etherification/homopolymerization reactions are not significant except under certain reaction conditions like high cure temperatures, high conversion,<sup>30,31</sup> and in the presence of an excess of epoxides. However, for thin DGEBA–DDM films (thickness < 160 nm), the etherification/homopolymerization reactions take place in the sublayer although cure temperature does not exceed 110 °C and conversion in epoxides is only 0.7. Figure 8 plots the percentage of epoxides in the sublayer

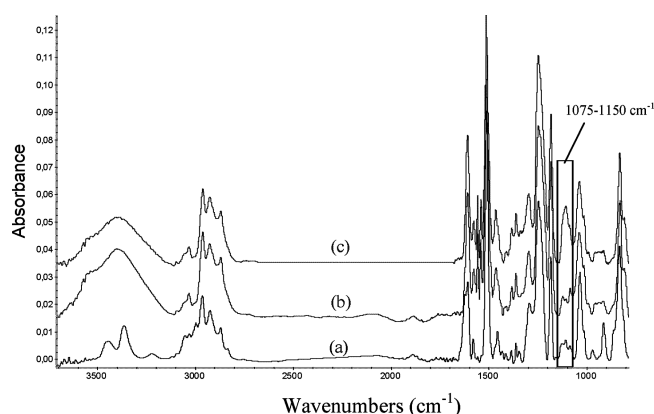


**Figure 7.** IRRAS spectra for epoxy/amine films on oxidized wafer: (a) before curing, (b) after curing (stage 1) for film thickness  $\sim 200$  nm, and (c) after curing (stage 1) for film thickness  $\sim 100$  nm.

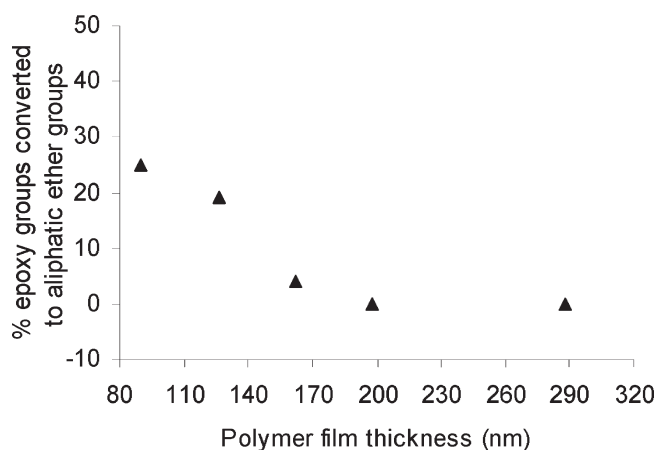


**Figure 8.** Percentage of epoxy functions converted to aliphatic ether in the sublayer during curing (according to the stage 1, i.e., without postcure at 180 °C) as a function of the film thickness.

converted to aliphatic ether groups as a function of the film thickness.

In most cases, addition of an amine in two steps is the most predominating processing in DGEBA–DDM systems. Nevertheless, for bifunctional epoxy this chain-growth polymerization side reaction is limited before complete primary amines consumption at low temperature.<sup>32</sup>

The activation energies of homopolymerization and etherification are almost 170 and 100 kJ/mol, respectively,<sup>33</sup> whereas the activation of primary amine–epoxy reaction is also 120 kJ/mol<sup>34</sup> in a nonautocatalytic process. This last value could be reduced to 70 kJ/mol in the presence of HX impurities at the beginning of the reaction. Taking into account the role of surface acidity of the wafer promoting by silanols on the epoxide rings, the primary amine–epoxy reactions as well as etherification between substrate and epoxide excess should be catalyzed<sup>35</sup> and bring about strongly chains mobility reduction near the substrate. Different studies<sup>11,16</sup> have also shown strong binding between epoxides in excess and the substrate surface limited to 1–5 nm thick. Furthermore, we notice that the amount of epoxide functions converted into aliphatic ethers in the sublayer is similar to the average excess of epoxides present in the sublayer before curing



**Table 1.** Comparison of Epoxy Groups Excess Present in the Sublayer before Curing, with the Amount of Epoxy Groups Converted to Aliphatic Ether in the Sublayer during Curing

film thickness (nm)	epoxy excess before curing (%)	epoxy converted to ether during curing (%)
126	12	19
90	23	25

takes as reference (Table 1). Then, increasing epoxy excess in the sublayer along with the mobility reduction and catalytic effects likely due to surface substrate favor reactions of etherification at low conversion rate.<sup>36</sup> These last are not only limited to a few nanometers but spreads out all over the sublayer. Indeed, Li and Simon<sup>37</sup> pointed out the silanols surface effect on the curing acceleration in controlled glass nanopores assigning the whole network until 280 nm range. Because of epoxide/silanol ratio increases as the film thickness decreases, etherification reaction is accelerated for thinnest films.

In the case of epoxy excess, Matejka<sup>32</sup> adds that intramolecular cyclization of DGEBA with secondary aromatic amine is preventing by the DGEBA-DDM stiffness but does not deny the intermolecular etherification reactions. Sherman<sup>38</sup> formulates model epoxy thermosets with different excess of epoxy and adds a specific catalyst in order to control etherification avoiding chain extension by epoxy homopolymerization. He demonstrates that network branched by etherification increasing linearly until an epoxide excess of 30% as it is observed in the sublayer of our systems inducing glass transition increase and a more heterogeneous network. These results suggest that the excess of epoxides groups, initially present in the sublayer for film thicknesses below 160 nm, is mainly consumed by etherification during curing.

Even if in this study we did not also attempt to distinguish whether the etherification is intermolecular (cross-linking) or intramolecular (cyclization) in nature, the dependency of the excess epoxides on the amount of aliphatic ethers created as well as the glass transition increase strengthens the hypothesis of intermolecular cross-linking of epoxy. This may be important in terms of cross-link density and resulting thermomechanical properties. Indeed, these etherification reactions reduce free volume induced by dangling epoxy molecules or rings and contribute to the increase of the observed sublayer  $T_g$  which is linked to the enhancement of the ether linkages as the film thickness decrease. As we had observed in thin films, Meyer<sup>28</sup> had shown that an increase of 15%–20% epoxides consumption by etherification in an epoxy-rich formulation ( $r \sim 0.8$ ) induced a 15 °C increase on the glass transition temperature. In thin films, we also notice a strong increasing dependency of aliphatic ether formation on the glass transition temperature.

**Confinement Effect on the Glass Transition Temperature of the Sublayer Cured at 110 °C.** To compare deviation in sublayer properties ascribed to side reactions,  $r = 0.8$  and  $r = 1$  amine/epoxy bulk samples were prepared according to the same thin films curing schedule (stage 1). However, to obtain a conversion of epoxy and primary amine of 0.54 and 0.57 for both samples, a postcure at 110 °C during 30 min is needed for the sample prepared in epoxy excess. Etherification reactions are not observed in these bulk samples. The glass transition temperatures measured by  $\mu$ TA (Table 2) are  $110 \pm 7$  °C ( $r = 0.8$  bulk sample) and  $140 \pm 7$  °C ( $r = 1$  bulk sample). Compared to

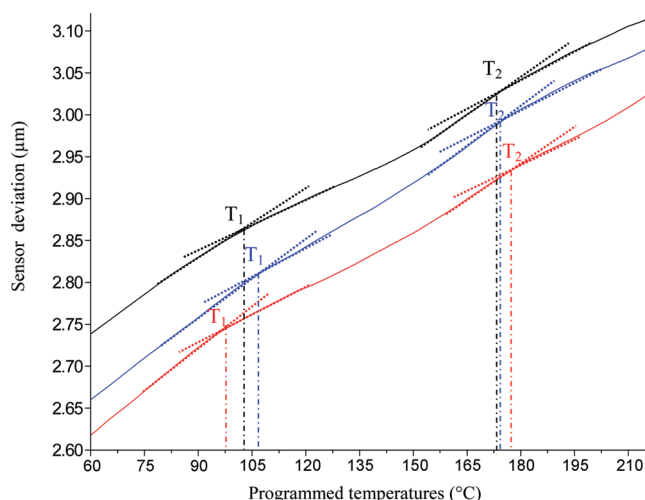
**Table 2.** Comparison of  $T_g$  in the Sublayer and the  $T_g$  of the Bulk Samples According to the Same Amine/Epoxy Ratio and Amine Conversion

amine/epoxy ratio	$T_g$ (°C)	
	in bulk	amine/epoxy ratio
$r = 0.8$	$110^a/130^b$	$165^c$
$r = 1$	140	143

<sup>a</sup> Without etherification. <sup>b</sup> With etherification. <sup>c</sup> With etherification at low curing temperature.

**Table 3.** Amine/Epoxy Ratio ( $r$ ) before Cure and after the First Cure Schedule (Stage 1) in the Sublayer versus the Film Thickness

thickness (nm)		$r$		
		before cure	after stage 1	
upper layer	sublayer	upper layer	sublayer	sublayer
30	60	2	0.72	1.10
30	96	2	0.86	1.09
30	132	2	0.93	1.00
30	168	2	0.97	0.86
30	186	2	0.99	0.90
30	222	2	1.01	0.91
30	258	2	1.03	0.94

**Figure 9.** Sensor height position response versus temperature for thin films postcured 2 h at 180 °C of different thicknesses: (a) 126, (b) 160, and (c) 200 nm.

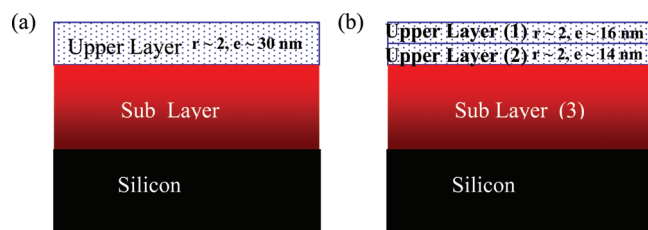
the glass transition temperatures of equivalent bulk samples at the same amine conversion without etherification, the influence of epoxy side reactions in the sublayer network on the measured glass transition temperature increase along with the etherification is confirmed.

Moreover, according to amine/epoxy ratio close to 1 at the same conversion rate without strong etherification in the sublayer, no deviation on the glass transition temperature between thin layer and bulk sample can be observed. First, it does not

mean that, as mentioned by Lenhart,<sup>11</sup> a glassy layer at the substrate interface associated with a local increase of  $T_g$  does not exist, but the ratio of this glassy layer versus the sublayer thickness is too small to arise this effect. Second, even though covalent bonds may exist between silicon substrate and the polymeric network, we do not measure a high glass transition enhancement as we had observed for the thickest films when we had grafted dense aminosilane layer on the substrate,<sup>17</sup> probably because their limited number. Third, the upper layer with a lower cross-link density could however forward its high mobility to the sublayer. This cooperative effect probably occurs, but it is limited to few nanometers and therefore moderately impacts the glass transition by a deviation of less than 10 °C,<sup>39</sup> which remains within the experimental errors. All these interface effects even if they occur do not seem to strongly modify the average glass transition temperature of the sublayer versus the bulk samples one for thicknesses above 160 nm. These experimental results and the corresponding former statistical models on epoxy—aromatic amine system with slow etherification limit from Gupta<sup>40</sup> or Tsou<sup>41</sup> bring out the importance of the etherification reactions especially on the increase glass transition temperature. Thereby, using tuned amine/epoxy composition in stratified thin films controlling amine—epoxy reactions beside etherification allows us to assign the input of the ether bonds versus epoxy—amine bonds on the network glass transition temperature.

**Effect of Postcure on the Glass Transition Temperature of the Sublayer.** After the first cure schedule at 110 °C named stage 1, the epoxy excess in the sublayer is supposed to have completely

**Scheme 1. Stratified Layer of Thin DGEBA DDM Film with (a) Upper Layer of 30 nm and Amine/Epoxy Ratio  $\sim 2$  and (b) Upper Layer Fictively Divided in Two Layers of 16 nm (1) and 14 nm (2) at the Same  $r \sim 2$  before Postcure at 180 °C<sup>a</sup>**



<sup>a</sup>Upper layer amines (2b) and sublayer amines and epoxides (3b) undergo postcuring.

**Table 4. Amine/Epoxy Ratio ( $r'$ ) before Postcure at 180 °C in the Fictive New Sublayer (2 + 3) Composed of a Fraction of the Upper Layer (2) and the Sublayer (3) after Stage 1 Curing versus the Film Thickness<sup>a</sup>**

thickness (nm)			after stage 1					before stage 2
			conversion in the sublayer (3)		upper layer (2)	sublayer (3)		$r'$
upper layer (1)	upper layer (2)	sublayer (3)	epoxy	amine	amine (mol)	amine (mol)	epoxides (mol)	sublayer (2 + 3)
16	14	60	0.70	0.55	$1.0497 \times 10^{-9}$	$1.5291 \times 10^{-9}$	$2.7865 \times 10^{-9}$	1.85
16	14	96	0.66	0.57	$1.0497 \times 10^{-9}$	$2.7211 \times 10^{-9}$	$4.9723 \times 10^{-9}$	1.52
16	14	132	0.55	0.51	$1.0497 \times 10^{-9}$	$4.4826 \times 10^{-9}$	$8.9970 \times 10^{-9}$	1.23
16	14	168	0.48	0.54	$1.0497 \times 10^{-9}$	$5.5865 \times 10^{-9}$	$1.2984 \times 10^{-8}$	1.02
16	14	186	0.47	0.51	$1.0497 \times 10^{-9}$	$6.6386 \times 10^{-9}$	$1.4768 \times 10^{-8}$	1.04
16	14	222	0.50	0.54	$1.0497 \times 10^{-9}$	$7.6546 \times 10^{-9}$	$1.6410 \times 10^{-8}$	1.06
16	14	258	0.51	0.52	$1.0497 \times 10^{-9}$	$9.2733 \times 10^{-9}$	$1.8695 \times 10^{-8}$	1.10

<sup>a</sup>The dimensions of the sample are 0.8 × 0.8 mm.

reacted inducing aromatic—aliphatic ether linkages. Therefore, the sublayer amine/epoxy ratio is close to 1 whatever the film thickness (Table 3). These films were postcured 2 h at 180 °C, stage 2, to complete epoxy reactions which are confirmed by FT-IRRAS spectra.

The L-TA measurements made on thin supported films after postcuring with different thicknesses are shown in Figure 9. Two glass transition temperatures are still observed for each sample. The first one remains close to  $104 \pm 6$  °C, and the second one is roughly  $177 \pm 6$  °C whatever the film thickness.

The higher  $T_g$  (i.e., the  $T_g$  of the sublayer) increases from 140–166 to 180 °C and no more depends on the film thickness. The lower glass transition temperature, more or less constant after this additional cure, is ascribed to the upper layer with a constant amine/epoxy ratio ( $\sim 2$ ). Its thickness is reduced to 16 nm for all the samples. This upper layer properties being constant after postcure, we assume that epoxy of the sublayer and a fraction of the amine excess from the former upper layer (observed after stage 1) react during postcuring. The polymer film after stage 1 has been divided fictively into three layers as it can be depicted in Scheme 1.

Thicknesses of layers 1 and 2 are respectively 16 and 14 nm and are composed of unreacted amines without anymore free epoxy. Layer 3 matches with the sublayer after stage 1 (Table 3). Using the conservation of matter in the whole film allows us to

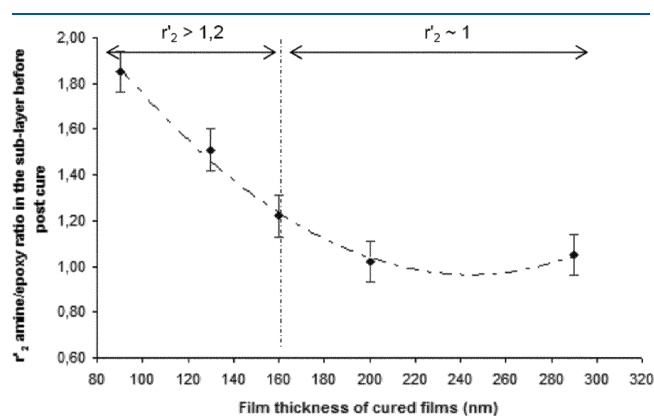


**Figure 10.** Amine/epoxy ratio of primary amine—epoxy functions potentially react during postcuring at 180 °C in the underlayer as a function of the film thickness.

estimate the average composition of amines and epoxides free to react before stage 2 versus the film thickness (Table 4).

The thinner the film is, the higher the amine/epoxy ratio is in the layers which undergo postcuring reactions as shown in Figure 10.

After postcure at 180 °C for 2 h, primary amine–epoxy conversion and ether bonds in these sublayers (2 + 3) are respectively 80%, 100%, and 20% for each film thickness (Figure 11).

As already mentioned in bulk system, postcure above 150 °C, high conversion rate<sup>30,31</sup> and epoxy excess promote etherification. In thin films, etherification side reactions are all the more as important as the amine/epoxy ratio is small. At high cure temperature, the main reactions in the sublayer are noticed between amines and epoxides for the thinnest films (<160 nm), whereas additional etherification reaction for thicker films is observed.

Finally, even if the chemical pathway is different in the sublayer according to the films thickness and relative stoichiometry, the conversion rate of amine, epoxide, and the average ether bonds in

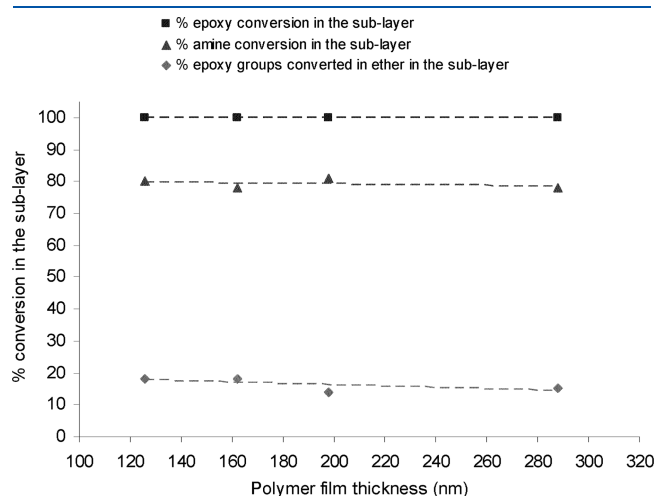


**Figure 11.** Percentage conversion of epoxy and amine groups in the sublayer, and percentage of epoxy groups converted in ether in the sublayer, as a function of the film thickness after postcure at 180 °C.

the sublayer of the totally cured films are equivalent for all the film thicknesses. The sublayer glass transition temperature of these films is also constant whatever the films thickness and equivalent to the bulk sample glass transition temperature with epoxy totally converted (i.e., DGEBA–DDM cured at 180 °C) as depicted in Scheme 2.

Contrary to many studies<sup>37,39,42</sup> on nanoconfinement which usually have highlighted a  $T_g$  depression according to an increase in chain stiffness or in epoxy conversion, the glass transition temperature still increases until 100% epoxy conversion and reaches the bulk glass transition temperature. Moreover, these interphases are not thin enough or the cooperatively rearranging region does not become sufficiently small, to result in a loss in the interphase behavior as can it be described in high cross-linked nanocomposites usually ascribed to a disruption of the dense network with the filler.<sup>39</sup> Therefore, the thinnest films partially cured with constant amine conversion exhibit a linear  $T_g$  enhancement with the epoxy conversion which can be mainly ascribed to ether bonds increase (Figure 12).

The network structure of the sublayer in DGEBA–DDM thin films seems to be stronger affected by both the substrate surface chemistry (side reactions becoming predominant at low temperature, interactions, or grafting onto the surface) and the amine segregation intensity at air/polymer interface (imbalance stoichiometry in the sublayer) than network confinement effect on

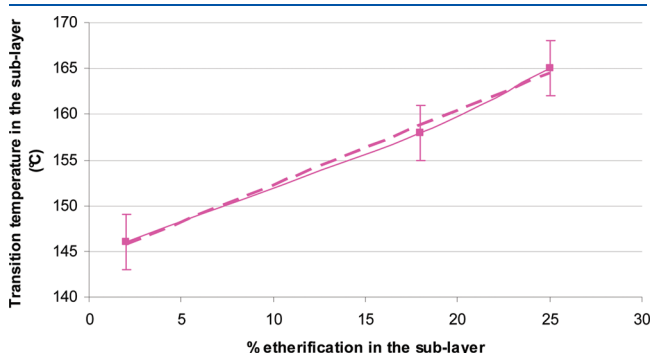
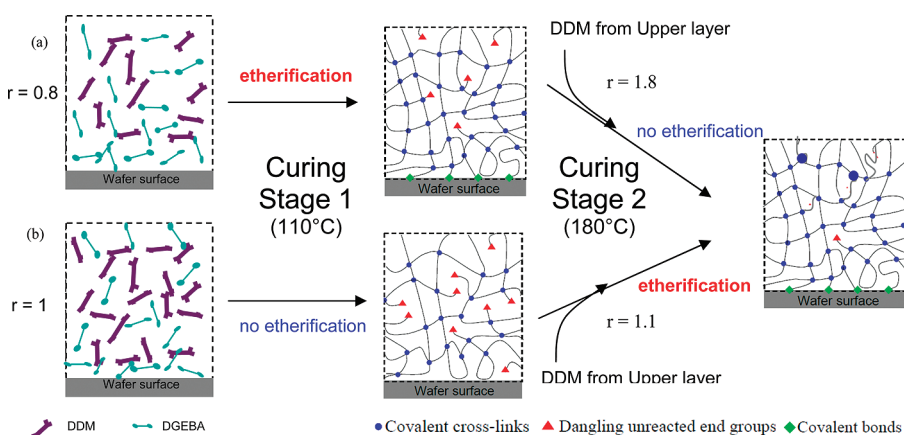


**Figure 12.** Evolution of the transition temperature as a function of the etherification in the sublayer.

**Scheme 2. Modification on the Amine/Epoxide Ratio in the Sublayer of a DGEBA–DDM Thin Films According to Its Thickness Induce Different Amine–Epoxy Chemical Pathways during Curing and Promote Etherification at Low Temperature in Epoxides Excess or at High Temperature in Stoichiometric Composition**



the glass transition temperature of partially and totally cured epoxy–amine thin films. Therefore, deviation of the thin film network formation mechanism from the bulk afford us to claim that knowledge of the sublayer off stoichiometry is not sufficient to predict its  $T_g$  from that obtained from an equivalent epoxy–amine bulk system partially cured at the same conversion rate. Indeed, we noticed that reactive components stratification and diffusion between asymmetric interfaces during curing modify chemical pathways as mentioned by Williams.<sup>43</sup> This phenomenon leads experimental difficulty in obtaining absolutely identical network chemical structure in thin film as compared with bulk sample for the same conversion rate. According to off stoichiometry, this means that asymmetric geometry of the cross-linked system and detailed catalysis reaction mechanisms must be carefully taken into account in any experimental studies, especially in thermal properties simulations of cross-linked network thin films or nanocomposites. The key parameter in defining the glass transition remains in a first step the network cross-link density,<sup>44</sup> and microthermal analysis is a convenient technique to obtain glass transition temperature at local scale in relation with the network density. Although the conditions of these preliminary characterizations and experimental limits mentioned above did not totally allow excluding specific effect of the substrate on the glass transition temperature, they already provide some insightful results regarding the dependence of etherification amount on the resulting glass transition temperature increase.

The next step forward in this work will focus on the way to tune toward the formation of desired interface between substrate and polymer network in thin films at the same cross-link density in order to establish fine relationships between the glass transition temperature and the chemical structure of the network with or without etherification. This might bring deeper understanding not only of direct relationships between chemical structures of the network and the  $T_g$  beside equivalent structure of bulk samples<sup>13,14</sup> but also by reducing thickness of the films to determine potentially confinement effect.

## CONCLUSION

In summary, although the segregation phenomena of reactive components and potential side reactions have been involved in explanations of glass transition temperature deviation in nanocomposites, this is the first direct evidence of a quantitative relationships between etherification, induced by phase segregation, and glass transition temperature deviation at interface. Because of the amine migration to the air/film interface is approximately constant whatever the thickness of polymer films and since the cross-linking and macromolecular mobility at the air/network interface are unaffected by the surface substrate and the film thickness, the important role of the amine–epoxy imbalance stoichiometry and the surface substrate catalysis on etherification at low temperature are demonstrated. Etherification enhancement with decreasing thickness of epoxy–amine cured film results in substantial increase of  $T_g$ . When off stoichiometry is limited, etherification probably only occurs near the surface substrate in a few nanometer range. It is not sufficient to enhance the polymer network average glass transition for sublayer thickness above 100 nm.

To our knowledge, the relationships between the modelization of these networks vertically nanostructured with strong deviation of the network formation mechanism beside the bulk

and the resulting glass transition temperature during curing do not exist. So, this sample geometry is a convenient way to control the amine/epoxy ratios at nanoscale tuning to a desired chemical structure of the network (ether bonds versus secondary and tertiary amines in the network). Our results should provide a driving force to future theoretical work in this area. Moreover, no evidence of confinement effect seems to occur in these thin films geometry. By reducing the films thickness, it is an open opportunity to distinguish the influence of confinement effect and network structure on the thermoset thin film glass transition temperature. A future study on this topic is currently under

## ASSOCIATED CONTENT

**S Supporting Information.** Figures S1–S4. This material is available free of charge via the Internet at <http://pubs.acs.org>. progress.

## AUTHOR INFORMATION

### Corresponding Author

\*E-mail: [pascal.carriere@univ-tln.fr](mailto:pascal.carriere@univ-tln.fr).

## ACKNOWLEDGMENT

This work was supported by a doctoral fellowship to Sandra Onard from the French Ministry of Research.

## REFERENCES

- (1) Fryer, D. S.; Nealey, P. F.; et al. *Macromolecules* **2000**, *33*, 6439.
- (2) Jones, F. R. *Key Eng. Mater.* **1996**, 116–117, 41.
- (3) DiBenedetto, A. T. *Mater. Sci. Eng. A* **2001**, *302*, 74.
- (4) Wang, X.; Zhou, W. *Macromolecules* **2002**, *35*, 6747.
- (5) Li, Q. X.; Simon, S. L. *Macromolecules* **2008**, *41*, 1310.
- (6) Tsui, O. K. C.; Zhang, H. F. *Macromolecules* **2001**, *34*, 9139.
- (7) Fakao, K.; Miyamoto, Y. *Phys. Rev. E* **2000**, *61*, 1743.
- (8) Wallace, W. E.; van Zanten, J. H.; Wu, W. L. *Phys. Rev. E* **1995**, *52*, 3329.
- (9) Keddie, J. L.; Jones, R. A. L.; Cory, R. A. *Europhys. Lett.* **1994**, *27*, 59.
- (10) Fryer, D. S.; Peters, R. D.; Kim, E. J.; Tomaszewski, J. E.; de Pablo, J. J.; Nealey, P. F.; White, C. C.; Wu, W. L. *Macromolecules* **2001**, *34*, 5627.
- (11) Lenhart, J. L.; Wu, W. *Macromolecules* **2002**, *35*, 5145.
- (12) Drzal, L. T. *Adv. Polym. Sci.* **1986**, *75*, 1.
- (13) Palmese, G. R.; McCullough, R. L. *J. Appl. Polym. Sci.* **1992**, *46*, 1863.
- (14) Palmese, G. R.; McCullough, R. L. *Composites, Part A* **1999**, *30*, 1.
- (15) Beck, T. N. C.; McKnight, S. H.; Palmese, G. R. *Proc. Am. Chem. Soc.: Polym. Mater. Sci. Eng.* **1997**, *77*, 640.
- (16) Yim, H.; Kent, M.; et al. *Macromolecules* **1999**, *32*, 7932.
- (17) Carriere, P.; Onard, S.; Mallarino, S. *Surf. Interface Anal.* **2009**, *41* (11), 858.
- (18) Tillman, M. S.; Takatoya, T.; et al. *J. Therm. Anal. Calorim.* **2000**, *62*, 599.
- (19) Habler, R.; Muhlen, E. *Thermochim. Acta* **2000**, *361*, 113.
- (20) Price, D. M.; Reading, M.; et al. *Thermochim. Acta* **1999**, *332* (2), 143.
- (21) Price, D. M.; Reading, M.; et al. *Eur. Ed.* **1998**, *53*, 21.
- (22) Hong-Bo, L.; Nagaiyanallur, V.; et al. *J. Phys. Chem. A* **2008**, *112*, 12372.
- (23) Christopher, J. G.; Glenn, R. H.; et al. *Anal. Chem.* **1994**, *66*, 1015.
- (24) Van Assche, G.; Ghanem, A.; et al. *Polymer* **2005**, *46*, 7132.



- (25) Hester, J. F.; Banerjee, P.; et al. *Macromolecules* **1999**, 32, 1643.
- (26) Hopkinson, I.; Kiff, F. T.; et al. *Macromolecules* **1995**, 28, 627.
- (27) Mundra, M. K.; Donthu, S. K.; et al. *Nano Lett.* **2007**, 7, 713.
- (28) Meyer, F.; Sanz, G.; et al. *Polymer* **1995**, 36, 1407.
- (29) Gupta, V. B.; Drzal, L. T.; et al. *Polym. Eng. Sci.* **1985**, 25, 812.
- (30) Mijovic, J.; Wijaya, J. *Polymer* **1994**, 35, 2683.
- (31) Chiao, L. *Macromolecules* **1990**, 23, 1286.
- (32) Matejka, L. *Macromolecules* **2000**, 33, 3611.
- (33) Sbirrazzuoli, N.; Mitililu-Mija, A.; et al. *Thermochim. Acta* **2006**, 447, 167.
- (34) Apicella, A.; Nicolais, M. I. *J. Appl. Polym. Sci.* **1984**, 29, 2083.
- (35) Jullien, H.; Petit, A.; et al. *Polymer* **1996**, 37, 3319.
- (36) Varley, R. J.; Heath, G. R.; et al. *Polymer* **1995**, 36, 1347.
- (37) Li, Q. X.; Simon, S. L. *Macromolecules* **2009**, 42, 3573.
- (38) Sherman, C. L.; Zeigler, R. C.; et al. *Polymer* **2008**, 49, 1164.
- (39) Putz, K. W.; Palmeri, M. J.; Cohn, R. B.; Andrews, R.; Brinson, L. C. *Macromolecules* **2008**, 41, 6752.
- (40) Gupta, A.; Macosco, C. J. *J. Appl. Polym. Sci.* **1990**, 28, 2585.
- (41) Tsou, A.; Peppas, N. J. *J. Appl. Polym. Sci.* **1988**, 26, 2043.
- (42) Ellison, C. J.; Mundra, M. K.; Torkelson, J. M. *Macromolecules* **2005**, 38, 1767.
- (43) Riccardi, C. C.; Williams, R. J. J. *J. Appl. Polym. Sci.* **1993**, 31, 389.
- (44) Hale, A.; Macosko, C. W.; et al. *Macromolecules* **1991**, 24, 2610.